Available online at www.sciencedirect.com
SCIENCE DIRECT®
Journal of Hydrology 283 (2003) 218–224
Journal of Hydrology
www.elsevier.com/locate/jhydrol

Addendum to overland flow to and through a segment of uniform resistance

W.L. Hogarth[a,*], J.-Y. Parlange[b], C.W. Rose[c]

[a]Faculty of Science and Information Technology, The University of Newcastle, Callaghan, NSW 2308, Australia
[b]Department of Biological and Environmental Engineering, Riley-Robb Hall, Cornell University, Ithaca, NY 14853, USA
[c]Faculty of Environmental Sciences, Griffith University, Nathan, QLD 4111, Australia

Received 28 November 2002; accepted 9 July 2003

Abstract

The St Venant equation is used to model the steady flow of water on a low slope through a grass buffer strip represented by beds of nails of various densities. The analytical solution is obtained both for flow upstream and within the buffer strip. Solution only requires the boundary conditions far upstream to be given and no curve fitting of parameters. The sensitivity of the solution to uncertainty in the measured boundary conditions and the effect of the theoretical resistive flow equation used are explored. Differences are observed between experimental observations and the theory but these are likely to be due to the presence of turbulent waves at the surface of the flow which are not part of the model.

Keywords: Uniform resistance; Buffer strips; Steady flow

1. Introduction

The use of vegetative buffer strips alongside streams to reduce the amount of pollution carried downstream through sediment and nutrient loading has been of recent scientific interest (Kemper et al., 1992; Landry and Thurow, 1997; Hairsine, 1996; Magette et al., 1989; Dabney et al., 1995; Munoz-Carpera et al., 1999). The buffer strips act as resistive elements to overland flow and modify the hydrology affecting the deposition of sediment and hence nutrient movement (Barfield et al., 1979; Flanagan et al., 1989; Dabney et al., 1995; Ghadiri et al., 2000, 2001).

Rose et al. (2002) developed a model of steady flow through a buffer strip represented by nail beds of various densities. The model divided the flow into four regions. This is represented in Fig. 1. The two regions of particular interest are firstly the zone between the hydraulic jump and the flow resistive element, and secondly the area within the nail bed. The other two regions show horizontal flows of depth D_1. Experiments were undertaken over an impermeable surface with a range of low slopes, the results were adequately modeled using several simplifying assumptions and curve fitting. In the following a purely analytical solution is presented both for flow through the nail bed and in the region of hydraulic

* Corresponding author.
E-mail address: bill.hogarth@newcastle.edu.au (W.L. Hogarth).

0022-1694/$ - see front matter © 2003 Elsevier B.V. All rights reserved.
doi:10.1016/S0022-1694(03)00268-3

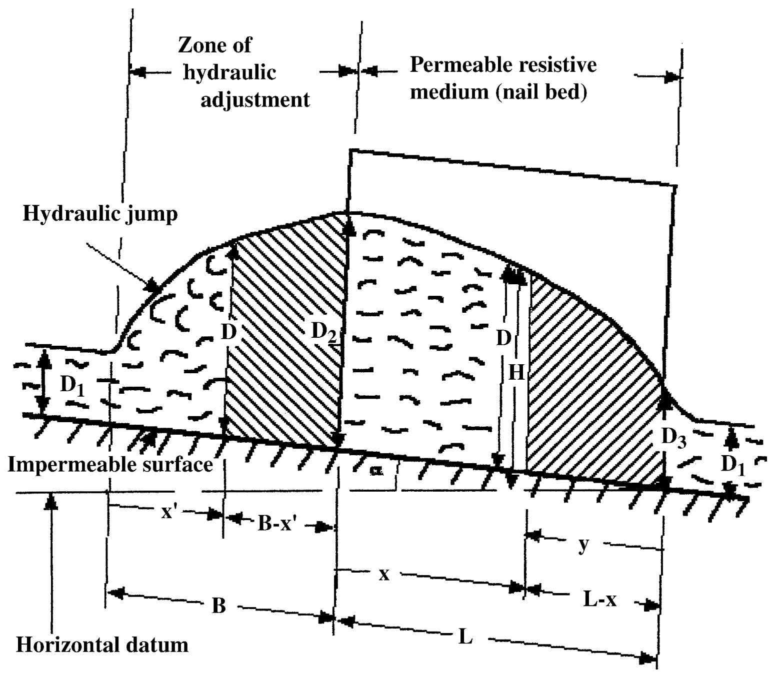

Fig. 1. Representation of the steady flow over an impermeable surface to and through a region of uniform resistive medium. Symbol definitions are given in the text and Appendix A.

adjustment that is entirely based on the St Venant equations and requires no curve fitting. Only the boundary conditions far upstream of the strip must be given.

This work assumes that the simulated buffer strip is spatially uniform in size and density, and that it does not change position or shape in response to flow. The water flowing is also assumed free of sediment or debris.

2. Model

In the following we follow closely Rose et al. (2002) and so will refer to their equations. Derivation of the equations can be found in their paper. The St Venant equation within the buffer strip (or nail bed), follows closely Eq. (22) in Rose et al. (2002) for small slopes (with the cos of the slope replaced by 1) or, here,

$$\frac{2}{D}\frac{\mathrm{d}D}{\mathrm{d}x} = \frac{2g\,\mathrm{S}D^2\theta - q^2 dC_\mathrm{d}N/\theta^2}{gD^3 - q^2/\theta} \tag{1}$$

where D is the depth of the water layer, x the distance down the flume, e.g. $x = 0$ at the entrance to the bed, $g = 9.81$ m/s^2, S is the slope, C_d is the drag coefficient around a cylindrical nail of diameter d, (Nm^{-2}) is the density of nails, and

$$\theta = 1 - \pi\, d^2/4e^2 \tag{2}$$

is the overall porosity of the bed, with e the nail spacing in both horizontal directions i.e. x and perpendicular to it. All symbols are listed in the Appendix A. Here, rather than curve fitting C_d, we take the standard value $C_\mathrm{d} \sim 1.1$ for the present Reynold's number (Marks, 1951). Eq. (1) is easily integrated as

$$S\theta(x-L) = D - D_3 + \frac{D_3^3}{A^2}\ln\frac{D}{D_3} + \frac{A^3 - D_3^3}{2A^2} \times \ln\frac{A-D}{A-D_3} - \frac{A^3 + D_3^3}{2A^2}\ln\frac{D+A}{D_3+A} \tag{3}$$

with

$$A^2 = q^2 dC_\mathrm{d}N/\theta^3\, 2\mathrm{g}S. \tag{4}$$

D_3 is the depth at $x = L$ which is the end of the nail bed. D_3 cannot be lower than the critical depth given by Eq. (1) as

$$D_C^3 = q^2/\theta g \tag{5}$$

Far downstream of the strip the depth must return to the normal depth D_1 which is imposed far upstream of the strip (once the turbulence generated by the nails has dissipated). However, $D_C > D_1$, hence the lowest possible value which the flow can reach at $x = L$ (the length of the nail bed) is

$$D_3 = D_C, \tag{6}$$

which is taken in the following. From Eq. (3) the depth, D_2, at $x = 0$, the entrance to the strip is easily obtained. This value is then used to obtain D upstream of the strip. The depth obeys the St Venant equation

$$\frac{dD}{dx} = gS\frac{D^3 - D_1^3}{gD^3 - q^2} \tag{7}$$

which is essentially Eq. (26) of Rose et al. (2002) with the small correction of D_1^3 ensuring that $dD/dx = 0$ at $D = D_1$. Here D_1^3 represents the drag on the board. For $D < D_2$, Eq. (7) describes the profile until a shock appears at a depth D_S given approximately by

$$D_S/D_1 = 0.5\left(\sqrt{1 + 8q^2/gD_1^3} - 1\right), \tag{8}$$

as given in any modern hydrology textbook, e.g. Chow (1959) and Haan et al. (1994) for flow on a horizontal surface. Note that in sloping channels Chow (1959) suggested a corrected relation. However for the weak jumps considered here the values of D_s/D_1 predicted by Eq. (8) are in essential agreement with the experimental relations also given on Chow (1959) in his Fig. 15–20.

Eq. (7) is easily integrated with the boundary condition obtained from Eq. (3) namely

$$D = D_2 \text{ at } x = 0 \tag{9}$$

giving

$$Sx = D - D_2 + \frac{D_1}{3}\left(1 - \frac{q^2}{gD_1^3}\right)\left[\ln\frac{D - D_1}{D_2 - D_1} - \ln\frac{D^2 + DD_1 + D_1^2}{D_2^2 + D_2D_1 + D_1^2} - \sqrt{3}\,\mathrm{Arc\,tan}\frac{2D + D_1}{\sqrt{3}D_1} + \sqrt{3}\,\mathrm{Arc\,tan}\frac{2D_2 + D_1}{\sqrt{3}D_1}\right] \tag{10}$$

3. Results

Figs. 2–5 analyze experiments described in Rose et al. (2002). The measured values of S, q, D_1, d, e, N are given in Table 1 of that paper. Experimental observations and the theoretical results obtained from Eqs. (3) and (10) are given. Several observations can be made from these results.

The shapes of the observations are fairly well described by Eqs. (3) and (10). However, the predictions of water depth tend to be significantly below the observations. The fact that the predictions are below the observations should be expected. Within the hydraulic jump zone the water is very choppy due to the presence of turbulent waves or ‘rollers’ (Chow, 1959). The recording strip can only show the envelope of the maximum crest of the rollers over the time of the experiment, and as those are highly turbulent (Rose et al., 2002) we should add the amplitude of those rollers to the predictions of average depth in order to compare with the observations. This addition of 3–5 mm (the larger value being for the VHD experiments) makes the predictions indistinguishable from the observations. Of course as the rollers penetrate the nail bed their amplitude decreases, more rapidly for a high nail density, and so the choppy appearance of the surface is less pronounced as we approach the exit at $x = L$, as observed. As a result near $x = L$ observations are closer to the theoretical result of the average depth.

The observed position where D increases over D_1 is always close to the predicted shock position where, $D = D_S$ as given by Eq. (8). At that place instead of a discontinuous jump the depth increases very rapidly (this region is properly described as the hydraulic jump). Experimental uncertainty in S and

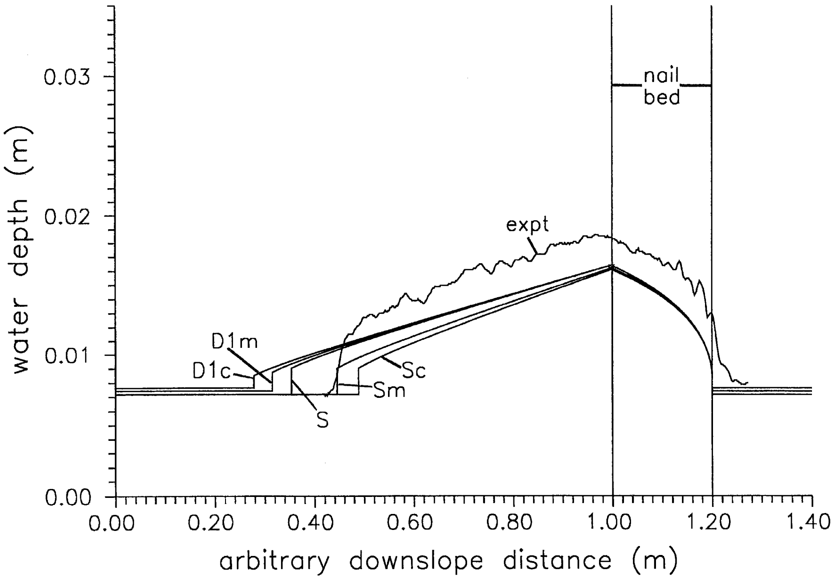

Fig. 2. Comparison of experimental and analytical results for steady water depth variation upstream and within a 0.2 m long high-density (2HD) nail bed. Flow is from left to right. Extent of nail bed is as shown. Parameter values are given in Table 1. Analytical curves are labeled according to the calculated value of S or D_1 from Manning's or Chezy's formula or the measured values of S and D_1 given by Rose et al. (2002) (Table 1).

D_1 has an effect on the position of the shock. In the Discussion section which follows we assess the sensitivity of the shock position to the uncertainty in the measurement of S and D_1.

4. Discussion

As in every experimental measurement there is some degree of uncertainty in both S and D_1. The

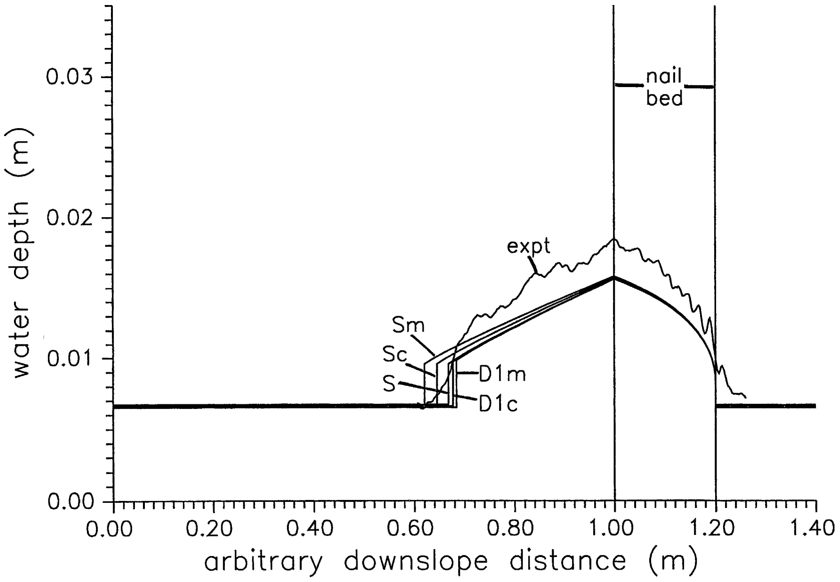

Fig. 3. Comparison of experimental and analytical results for steady water depth variation upstream and within a 0.2 m long, high density (3HD) nail bed (in a similar way to Fig. 2).

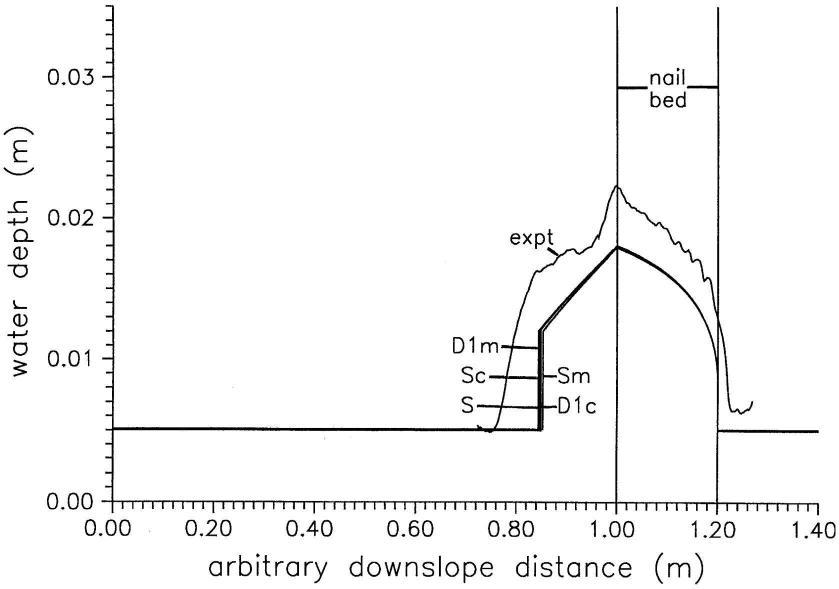

Fig. 4. Comparison of experimental and analytical results for steady water depth variation upstream and within a 0.2 m long, high density (4V HD) nail bed (in a similar way to Fig. 2).

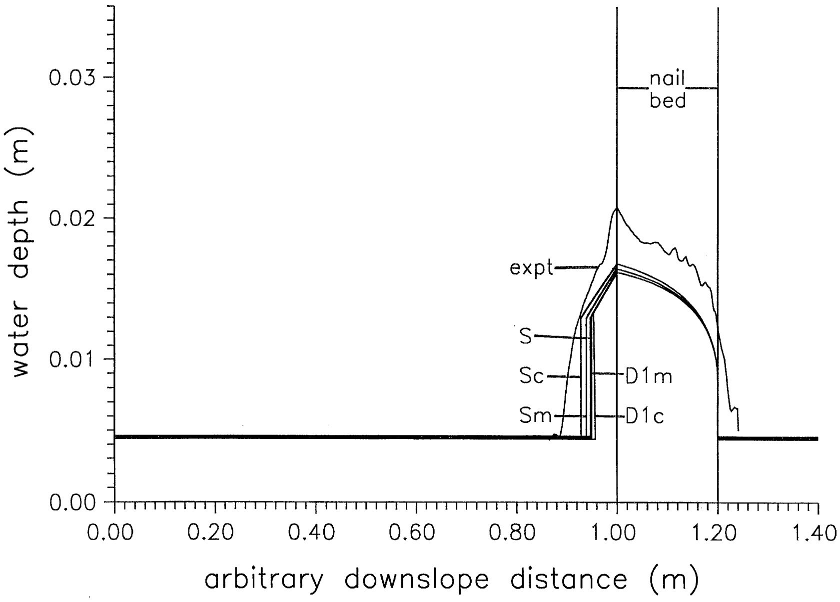

Fig. 5. Comparison of experimental and analytical results for steady water depth variation upstream and within a 0.2 m long, high density (5V HD) nail bed (in a similar way to Fig. 2).

Table 1
Experimental and calculated data for four experiments given in Rose et al. (2002)

Experiment	S	q	D_1	$D_1S^{0.3}$	$D_1S^{1/3}$	S_m	D_{1m}	S_c	D_{1c}
2HD	0.0100	2.27×10^{-3}	7.18×10^{-3}	1.804×10^{-3}	1.547×10^{-3}	0.01124	7.436×10^{-3}	0.01208	7.647×10^{-3}
3HD	0.0154	2.27×10^{-3}	6.73×10^{-3}	1.924×10^{-3}	1.674×10^{-3}	0.01395	6.533×10^{-3}	0.01467	6.622×10^{-3}
4V HD	0.0354	2.27×10^{-3}	5.10×10^{-3}	1.850×10^{-3}	1.652×10^{-3}	0.03516	5.090×10^{-3}	0.03371	5.018×10^{-3}
5V HD	0.0520	2.27×10^{-3}	4.60×10^{-3}	1.895×10^{-3}	1.717×10^{-3}	0.04950	4.535×10^{-3}	0.04594	4.414×10^{-3}

S: flume slope; q discharge rate per unit width; D_1: flow depth upstream of hydraulic jump; S_m: flume slope obtained from Manning's formula taking D_1 as measured; D_{1m}: D_1 obtained from Manning's formula taking S as measured; S_c and D_{1c} are similarly obtained using Chezy's formula.

effect of such uncertainty can be investigated using Manning's and Chezy's formula. Manning's formula gives

$$q = \frac{D_1^{5/3}S^{1/2}}{n} = \frac{(D_1S^{3/10})^{5/3}}{n} \qquad (11)$$

and Chezy's formula gives

$$q = CD_1^{3/2}S^{1/2} = C(D_1S^{1/3})^{3/2}. \qquad (12)$$

Since q is constant for all the experiments then in Manning's formula $D_1S^{0.3}$ should be constant as

Table A1
List of symbols

Symbol	Description	Defining equations/figures
Roman		
B	Length of zone of hydraulic adjustment	
C_d	Drag coefficient of a single nail	
d	Nail diameter	
D	Depth of water flow	
D_1	Depth of normal flow	Fig. 1
D_2	Depth of water at entry to the nail bed	Fig. 1
D_3	Depth of water of exit from the nail bed	Fig. 1
D_a	Average water depth over distance $(L-x)$ or y	Fig. 1
D_c	Critical depth of water at exit of nail bed	Eq. (5)
D_s	Depth of water at position of shock	Eq. (8)
e	Nail spacing	
g	Acceleration due to gravity	
H	Hydraulic head	Fig. 1
L	Length of nail bed	Fig. 1
N	Nail density (no. nails m^{-2})	
q	Unit discharge	
S	Bed slope = sin α	
V_2	Flow velocity with flow depth D_2	
V_a	Average flow velocity over distance $(L-x)$ or y	Fig. 1
x	Downslope distance measured from upstream face of the nail bed	Fig. 1
x'	Downslope distance measured from the commencement of the hydraulic jump	Fig. 1
y	Distance measured upslope from the downslope of the nail bed	Fig. 1
Greek		
α	Slope angle of the flow bed	Fig. 1
θ	Volumetric water content of flow within the nail bed	Eq. (2)
ν	Kinematic viscosity of water	
ρ	Water density	

should $D_1S^{1/3}$ in Chezy's formula irrespective of the values of n or C. Table 1 shows the results.

As shown in Table 1, $D_1S^{0.3}$ and $D_1S^{1/3}$ are not quite constant, indicating either the effect of error in measurements of D_1 and S, or some deficiency in the formulae. The effect of this uncertainty is investigated by using averaged values taken across the experiments, i.e. for $D_1S^{0.3}$, 1.868×10^{-3} and for $D_1S^{1/3}$, 1.6475×10^{-3} to obtain the last four columns in Table 1. For example, D_{1c} for experiment 2HD is obtained using $D_1S^{1/3}$, with average value 1.6475×10^{-3} and the value of S, 0.01 while S_m for experiment 2HD is obtained from $D_1S^{0.3}$, with average value 1.868×10^{-3} and the value of D_1, 7.18×10^{-3}.

Figs. 2–5 show the sensitivity of the position of the shock to the values of S and D_1. We note the following. Firstly, considering the overall variability in the shock position there is relatively little difference between the use of Chezy or Manning's equation. Secondly, taking S and D, as measured tends to predict an 'average' shock position. Finally, estimating S from either Chezy or Manning and the measured D_1, is somewhat better in predicting the position of the shock, especially for the lowest slope.

5. Conclusion

This addendum presents a theoretical approach to describing the steady flow of clear water through a buffer strip represented by nail beds of various densities. The theory clearly represents the physical features shown in the experiments. The position of the shock is sensitive to the choice of the slope S and original water depth far upstream D_1. At least one reason why the measured envelope of the maximum water depth exceeds prediction could be the presence of turbulent rollers.

The presence of sediment and debris in flowing water, and the non-uniformity and lack of rigidity characteristic of real world buffer strips adds further complications to experiment and theory.

Appendix A

Table A1.

References

Barfield, B.J., Tollner, E.W., Hayes, J.C., 1979. Filtration of sediment by simulated vegetation. I. Steady-stage flow with homogenous sediment. Transactions of ASAE 22 (5), 540–545.also see p. 548.

Chow, V.T., 1959. Open Channel Hydraulics, McGraw Hill, New York.

Dabney, S.M., Meyer, L.D., Harmon, W.C., Alonso, C.V., Foster, G.R., 1995. Depositional patterns of sediment trapped by grass hedges. Transactions of ASAE 38 (6), 1719–1729.

Flanagan, D.C., Foster, G.R., Neibling, W.H., Burt, J.P., 1989. Simplified equations for filter strip design. Transactions of ASAE 32 (6), 2001–2007.

Ghadiri, H., Hogarth, W.L., Rose, C.W., 2000. The effectiveness of grass strips for the control of sediment and associated pollutant transport in runoff. In: Stone, M., (Ed.), Role of Erosion and Sediment Transport in Nutrient and Contaminant Transfer, IAHS Publication No. 263, IAHS, Oxfordshire, UK, pp. 83–91.

Ghadiri, H., Rose, C.W., Hogarth, W.L., 2001. The influence of grass and porous barrier strips on runoff hydrology and sediment transport. Transactions of ASAE 44 (2), 259–268.

Haan, C.T., Barfield, B.J., Hayes, J.C., 1994. Design Hydrology and Sedimentology for Small Catchments, Academic Press, San Diego.

Hairsine, P.B., 1996. Comparing grass filter strips and near-natural riparian forests for buffering intense hillslope sediment sources. Proceedings of the First National Conference on Stream Management in Australia, 19–23 February 1996, Merrijig, Australia. Cooperative Research Centre for Catchment Hydrology, Monash University, Victoria, Australia, pp. 203–206.

Kemper, D., Dabney, S., Kramer, L., Dominick, D., Keep, T., 1992. Hedging against erosion. Journal of Soil and Water Conservation 47, 284–288.

Landry, M.S., Thurow, L.L., 1997. Function and design of vegetation filter strips: an annotated bibliography. Texas State Soil and Water Conservation Board Bulletin No. 97-1. P.O. Box 658, Temple, USA, p. 67.

Magette, W.L., Brinsfield, R.B., Palmer, R.E., Wood, J.D., 1989. Nutrient and sediment removal by vegetated filter strips. Transactions of ASAE 32 (2), 663–667.

Marks, L.S., 1951. Mechanical Engineers Handbook, 5th ed., McGraw Hill, New York.

Munoz-Carpena, R., Parsons, J.E., Gilliam, J.W., 1999. Modelling hydrology and sediment transport in vegetative filter strips. Journal of Hydrology 214, 111–129.

Rose, C.W., Hogarth, W.L., Ghadiri, H., Parlange, J.Y., Okom, A., 2002. Overland flow to and through a segment of uniform resistance. Journal of Hydrology 255, 134–150.